Correlation between α-particle preformation probability and the energy levels of parent nuclei

M. Ismail and A. Adel*
Physics Department, Faculty of Science, Cairo University, Giza, Egypt
(Received 24 April 2012; published 23 July 2012)

A realistic density-dependent nucleon-nucleon (NN) interaction with a finite-range exchange part which produces the nuclear matter saturation curve and the energy dependence of the nucleon-nucleus optical potential model is used to calculate the preformation probability, S_α, of α decay from Po isotopes to superheavy nuclei. The variation of S_α with the neutron number for the isotopes of Po, Rn, Ra, Th, and U elements is studied below and above the magic neutron number $N = 126$. We found a strong correlation between the behavior of S_α and the energy levels of the parent nucleus at and just below the Fermi level. S_α has a regular behavior with the neutron number if the neutron pair of α particles, emitted from adjacent isotopes, comes from the same energy level or from a group of levels, assuming that the order of levels in this group is not changed. Irregular behavior of S_α with the neutron number occurs if the levels of the adjacent isotopes change or holes are present in lower levels.

DOI: 10.1103/PhysRevC.86.014616 PACS number(s): 23.60.+e, 21.10.Tg, 21.10.Jx, 27.90.+b

I. INTRODUCTION

α decay is one of the most important decay modes for heavy and superheavy nuclei (SHN) [1]. It provides some reliable knowledge on nuclear structure [1–4]. It gives unique information on masses (via the decay energy Q_α) and excitation energies of the closely spaced excited and ground states, for which other common experimental methods are not yet possible. α decay also presents a useful tool for study of the spectroscopy of unstable nuclei [5], which is essentially connected with the phenomenon of α-cluster formation in decaying nuclei. In recent experiments, the investigation of α-decay chains of SHN is indispensable to the identification of new elements and isomeric states [6,7]. New synthesized superheavy elements such as Z = 107–113 have been successfully synthesized by the cold fusion reactions at GSI in Germany [1,8] and RIKEN in Japan [9], and elements 114–118 have also been synthesized by hot fusion reactions at Dubna in Russia [7,10–12]. Encouraged by these experimental achievements, extensive α-decay studies based on various models have been devoted to pursue a quantitative description of SHN.

The α-decay process is treated conventionally in the framework of the Gamow model [13] assuming a sub-barrier penetration of α particles through the barrier, caused by interactions between α particles and the daughter nucleus. Many effective theoretical approaches have been used to describe α decay, such as the generalized liquid-drop model [14], the density-dependent cluster model (DDCM) [15], the united model for α decay and α capture [16], and the Coulomb and proximity potential model [17], and all of them have been successful in reproducing the experimental data and also in predicting half-life values.

The absolute α-decay width is mainly determined by the α-cluster penetration probability, which can be obtained in terms of the well-known Wentzel-Kramers-Brillouin (WKB) semiclassical approximation [18]. Calculation of the penetration probability requires a reliable input of the α-nucleus interaction potential, which consists of both Coulomb repulsive and nuclear attractive parts. The Coulomb part is well known, but the nuclear part is less well defined. It is either introduced phenomenologically [19,20] (e.g., Woods-Saxon shape with adjusted parameters) or generated microscopically in some approximation using calculated nuclear densities [21,22] (e.g., double-folding model).

The most important problem of the α decay is how to estimate the preformation probability, or the so-called spectroscopic factor S_α, that the α particle exists as a recognizable entity inside the nucleus before its emission. It is very dependent on the structure of the states of the parent and daughter nuclei [23–25]. One needs a very large shell model basis to obtain the experimental values of the α-preformation probability. The combined shell and cluster model [26], which treats a large shell model basis up to the continuum states through the wave function of the spatially localized α cluster, explains the experimental decay width well . In these calculations the wave function is necessary, and it is not easy to extend the approaches for nuclei including more nucleons outside the double-magic core.

In the present work, the preformation factor, S_α, is extracted from the experimental α-decay half-life and the penetration probability is obtained from the WKB approximation in combination with the Bohr-Sommerfeld quantization condition. The potential barrier is numerically determined in the well-established double-folding model for both Coulomb and nuclear potentials. A realistic density-dependent M3Y interaction [27], based on the G-matrix elements of the Paris NN potential, has been used in the folding calculation. The local approximation for the nondiagonal one-body density matrix in the calculation of the exchange potential was included by using the harmonic oscillator representation of the nondiagonal density matrix of the α particle [28,29]. Moreover, we tried to correlate the behavior of S_α with the variation of the neutron number, N, for isotopes of $Z = 84$–92 elements with spins of adjacent odd-neutron-number isotopes.

*ahmedshosha200@yahoo.com

This paper is organized as follows. In Sec. II the double-folding model is introduced and the methods for determining the decay width, penetration probability, assault frequency, and preformation probability are presented. In Sec. III the calculated results are presented and discussed. The conclusion is given in Sec. IV.

II. THEORETICAL FRAMEWORK

In the density-dependent cluster model, the ground state of the parent nucleus is assumed to be an α particle interacting with the daughter nucleus. The total α-core potential is the sum of the nuclear, Coulomb, and centrifugal potentials and is given by [15,21]

$$V_{\rm T}(R) = \lambda\, V_N(R) + V_C(R) + \frac{\hbar^2}{2\,\mu}\frac{\left(\ell+\frac{1}{2}\right)^2}{R^2}, \qquad (1)$$

where the renormalization factor λ is the depth of the nuclear potential, R is the separation between the mass center of the α particle and the mass center of the core, and ℓ is the angular momentum carried by the α particle.

In the first order of the many-body theory, the microscopic α-nucleus potential can be evaluated as an antisymmetrized Hartree-Fock-type potential for the dinuclear system in the framework of the folding model based on the effective M3Y nucleon-nucleon (NN) interaction [29],

$$V = \sum_{i\in\alpha,\, j\in d} \left[\langle ij|\upsilon_D|ij\rangle + [\langle ij|\upsilon_{\rm Ex}|ji\rangle\right], \qquad (2)$$

where $|i\rangle$ and $|j\rangle$ are the single-particle wave functions of nucleons in the α and daughter nuclei, respectively. So, we fold in the nuclear density distributions of the two fragments with the realistic M3Y effective interaction. Here, υ_D and $\upsilon_{\rm Ex}$ are the direct and exchange parts of the effective NN interaction. The antisymmetrization of the dinuclear system is done by taking into account the so-called single-nucleon knock-on exchange effects (the interchange of nucleons i and j).

The direct term is local (provided that the NN interaction itself is local) and can be written in terms of the one-body spatial densities,

$$V_D(R) = \int {\rm d}\vec{r}_1 \int {\rm d}\vec{r}_2 \rho_\alpha(\vec{r}_1)\, \upsilon_D(\rho,\, E,\, s)\, \rho_d(\vec{r}_2), \qquad (3)$$

where s is the relative distance between a constituent nucleon in the α particle and one in the core nucleus. $\rho_\alpha(\vec{r}_1)$ and $\rho_d(\vec{r}_2)$ are, respectively, the density distributions of the α particle and residual core nucleus.

In all previous calculations of the α-particle decay processes, it is assumed that the exchange part of the NN interaction, $V_{\rm Ex}$, has a zero range [15,21,25,30]. By this assumption, one neglects antisymmetrization between the nucleons in the α-particle and the nucleons in the daughter nucleus, which is essential to satisfy the Pauli exclusion principle. Recently, the antisymmetrization of the dinuclear system is taken into account [31] but through more complicated calculations. If $V_{\rm Ex}$ is assumed to be zero ranged [$\upsilon_{\rm Ex}(s) = -V_0\,\delta(s)$], the second term in Eq. (2) becomes

$$V_{\rm Ex}(R) = -V_0 \int {\rm d}\vec{r}\, \rho_\alpha(\vec{r}+\vec{R})\, \rho_d(\vec{r}), \qquad (4)$$

which can be calculated more rapidly than $V_{\rm D}(R)$ given by Eq. (3). The exchange term is, in general, nonlocal. However, an accurate local approximation can be obtained by treating the relative motion locally as a plane wave [32,33],

$$V_{\rm Ex}(E,\, R) = \int {\rm d}\vec{r}_1 \int {\rm d}\vec{r}_2 \rho_\alpha(\vec{r}_1, \vec{r}_1+\vec{s})\, \rho_d(\vec{r}_2, \vec{r}_2-\vec{s}) \times \upsilon_{\rm Ex}(\rho,\, E,\, s) \exp\left[\frac{i\vec{k}(R)\cdot\vec{s}}{M}\right]. \qquad (5)$$

Here $k(R)$ is the relative motion momentum given by

$$k^2(R) = \frac{2\,\mu}{\hbar^2}\left[E_{\rm c.m.} - V_N(E,\, R) - V_C(R)\right], \qquad (6)$$

where μ is the reduced mass for the reacting nuclei, $E_{\rm c.m.}$ is the center-of-mass (c.m.) energy. $V_N(E,\, R) = V_D(E,\, R) + V_{\rm Ex}(E,\, R)$ and $V_C(R)$ are the total nuclear and Coulomb potentials, respectively. The folded potential is energy dependent and nonlocal through its exchange term and contains a self-consistency problem because k depends on V. The exact treatment of the nonlocal exchange term is complicated numerically, but one may obtain an equivalent *local* potential by using a realistic approximation for the nondiagonal density matrix (DM) [29,32]

$$\rho(\vec{r}, \vec{r}+\vec{s}) \simeq \rho\left(\vec{r}+\frac{\vec{s}}{2}\right) \hat{j}_1\left(k_{\rm eff}\left(\vec{r}+\frac{\vec{s}}{2}\right)s\right), \qquad (7)$$

with

$$\hat{j}_1(x) = 3\, j_1(x)/x = 3(\sin x - x\cos x)/x^3. \qquad (8)$$

The α particle is a unique case where a simple Gaussian can reproduce very well its ground-state density [34]. Assuming four nucleons to occupy the lowest $s\,\frac{1}{2}$ harmonic oscillator shell in ^{4}He, one obtains exactly the nondiagonal ground-state DM for the α particle as [29]

$$\rho_\alpha(\vec{r}, \vec{r}+\vec{s}) \simeq \rho_\alpha\left(\left|\vec{r}+\frac{\vec{s}}{2}\right|\right) \exp\left(-\frac{s^2}{4\,b_\alpha^2}\right). \qquad (9)$$

To accelerate the convergence of the density matrix expansion, Campi and Bouyssy [35] have suggested to choose, for a spherically symmetric ground-state density, the local Fermi momentum $k_{\rm eff}(r)$ in the following form:

$$k_{\rm eff}(r) = \left\{\frac{5}{3\rho(r)}\left[\tau(r) - \frac{1}{4}\nabla^2\rho(r)\right]\right\}^{1/2}. \qquad (10)$$

Using the extended Thomas-Fermi approximation, the kinetic energy density is then given by

$$\tau(r) = \frac{3}{5}\left(\frac{3\pi^2}{2}\right)^{2/3}\rho(r)^{5/3} + \frac{1}{3}\nabla^2\rho(r) + \frac{1}{36}\frac{|\vec{\nabla}\rho(r)|^2}{\rho(r)}. \qquad (11)$$

The first term in this expression stands for the Thomas-Fermi approximation, while the other two terms represent the surface correction.

One easily obtains the self-consistent and local exchange potential $V_{\rm Ex}$ as

$$V_{\rm Ex}(E,R) = 4\pi \int_0^\infty {\rm d}s\, s^2\, \upsilon_{\rm Ex}(\rho,E,s)\, j_0(k(E,R)s/M) \times \int {\rm d}\vec{y}\, \rho_d(|\vec{y}-\vec{R}|)\hat{j}_1(k_{\rm eff}(|\vec{y}-\vec{R}|)s) \times \rho_\alpha(y)\exp\left(-\frac{s^2}{4\,b_\alpha^2}\right). \quad (12)$$

$V_{\rm Ex}$ depends on the total potential, $V(R) = V_D + V_{\rm Ex} + V_C$, through the relative motion momentum given by Eq. (6). So, the problem of obtaining $V(R)$ is a self-consistent problem. The exchange potential, Eq. (12), can then be evaluated by an iterative procedure which converges very fast.

The NN interaction used in the α-decay calculations is usually an M3Y-Reid interaction with zero-range exchange part. This type of force is successful when heavy-ion interaction is dominated by strong absorption, i.e., when the elastic scattering data are sensitive to the potential only on the surface region. For α decay, the potential used in the calculations should correctly describe the bulk properties of the nucleus, as a part of the α-decay calculations depends on the value of interaction potential in the interior region. So we use, for the first time, a realistic NN interaction whose parameters reproduce consistently the equilibrium density and binding energy of normal nuclear matter as well as the density and energy dependence of the nuclear optical potential. The density-dependent M3Y-Paris effective NN force considered in the present work, BDM3Yn, has the factorized form [27]

$$\upsilon_D(\rho,E,s) = \left[11061.625\,\frac{e^{-4s}}{4\,s} - 2537.5\,\frac{e^{-2.5s}}{2.5\,s}\right] F(\rho)\,g(E), \quad (13)$$

$$\upsilon_{\rm Ex}(\rho,E,s) = \left[-1524.25\,\frac{e^{-4s}}{4\,s} - 518.75\,\frac{e^{-2.5s}}{2.5\,s} - 7.8474\,\frac{e^{-0.7072s}}{0.7072\,s}\right] F(\rho)\,g(E), \quad (14)$$

with the density and energy dependence, respectively,

$$F(\rho) = c(1-\gamma\rho^n), \quad (15)$$

$$g(E) = (1 - 0.003\,E_{\rm Ap}), \quad (16)$$

The parameters c, γ, and n are adjusted to reproduce normal nuclear matter saturation properties for a given equation of state for cold nuclear matter. For BDM3Y1, $c = 1.2521$, $\gamma = 1.7452$ fm^3, and $n = 1$, which generate a nuclear matter equation of state with the incompressibility value, $K =$ 270 MeV. $E_{\rm Ap}$ is the incident energy per projectile nucleon in the laboratory system.

The matter density distribution of the α particle is a standard Gaussian form, namely,

$$\rho_\alpha(r) = 0.4229\exp(-0.7024\,r^2). \quad (17)$$

The matter density distribution for the daughter nucleus can be described by the spherically symmetric Fermi function,

$$\rho_d(r) = \frac{\rho_0}{1+\exp\left(\frac{r-R_0}{a}\right)}, \quad (18)$$

where the value of ρ_0 has been fixed by integrating the matter density distribution equivalent to the mass number of the residual daughter nucleus A_d. The half-density radius, R_0, and the diffuseness parameter, a, are given by [21,36,37]

$$R_0 = 1.07A_d^{1/3}\ {\rm fm}, \quad a = 0.54\ {\rm fm}. \quad (19)$$

The renormalization factor λ, introduced to the nuclear part of the folding potential based on the M3Y interaction, is not an adjustable parameter, but it is determined separately for each decay by applying the Bohr-Sommerfeld quantization condition [38],

$$\int_{R_1}^{R_2} {\rm d}r \sqrt{\frac{2\,\mu}{\hbar^2}\,|V_T(r)-Q_\alpha|} = (2n+1)\,\frac{\pi}{2} = (G-\ell+1)\,\frac{\pi}{2}, \quad (20)$$

where the global quantum number $G = 20\,(N > 126)$ and $G = 18\,(82 < N \leqslant 126)$ [15]. Here, n expresses the number of nodes of the quasibound wave function of the α-nucleus relative motion. Q_α is the Q value of the α decay. R_i $(i = 1, 2, 3)$ are the three turning points for the α-daughter potential barrier where $V_T(r)|_{r=R_i} = Q_\alpha$.

In the framework of the preformed cluster model, the α-decay partial half-lifetime, $T_{1/2}$, of the parent nucleus is given in terms of the α-decay width, Γ, as

$$T_{1/2} = \frac{\hbar\ln 2}{\Gamma}. \quad (21)$$

The absolute α-decay width is mainly determined by the barrier penetration probability (P_α), the assault frequency (ν), and the preformation probability, the spectroscopic factor of the α cluster inside the parent nucleus (S_α), $\Gamma = \hbar\, S_\alpha\, \nu\, P_\alpha$. The barrier penetration probability, P_α, could be calculated as the barrier transmission coefficient of the well-known WKB approximation, which works well at energies well below the barrier:

$$P_\alpha = \exp\left(-2\int_{R_2}^{R_3} {\rm d}r \sqrt{\frac{2\mu}{\hbar^2}|V_T(r)-Q_\alpha|}\right). \quad (22)$$

The assault frequency of the α particle, ν, can be expressed as the inverse of the time required to traverse the distance back and forth between the first two turning points, R_1 and R_2, as [38]

$$\nu = T^{-1} = \frac{\hbar}{2\mu}\left[\int_{R_1}^{R_2} \frac{{\rm d}r}{\sqrt{\frac{2\mu}{\hbar^2}|V_T(r)-Q_\alpha|}}\right]^{-1}. \quad (23)$$

Finally, the spectroscopic factor (the preformation probability) of the α cluster inside the parent nucleus can then be obtained as the ratio of the calculated half-life, without S_α, to the experimental one [25,39]:

$$S_\alpha = T_{1/2}^{\rm cal}/T_{1/2}^{\rm exp}. \quad (24)$$

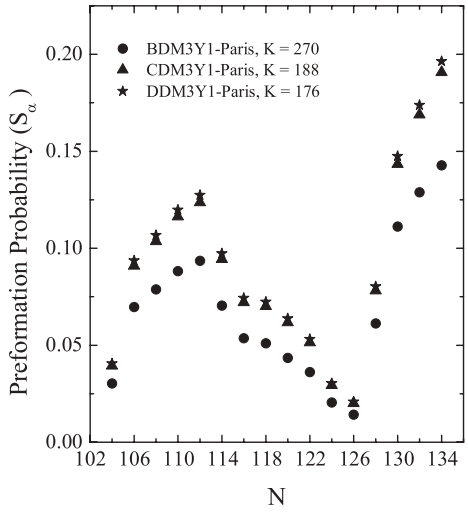

FIG. 1. Extracted α-preformation probability, S_α, for Po isotopes using three NN interactions with different compressibility coefficients, K, with the neutron number, N.

III. RESULTS AND DISCUSSION

Based on the realistic density-dependent effective BDM3Y1-Paris NN interaction, the half-lives of the ground state–to–ground state α decay of the even-even radioactive nuclei from Po isotopes to SHN have been calculated. The main effect of antisymmetrization under exchange of nucleons between the α and the daughter nuclei has been included in the folding model through the finite-range exchange part of the NN interaction. The implementation of the Bohr-Sommerfeld quantization condition in the WKB approach determines the renormalization factor λ of the nuclear potential separately for each decay. The value of λ, in the present calculations, ranges from 0.85 to 0.96, which is close to unity. The calculated total interaction potential, after adding the Coulomb part, is used to obtain the tunneling probability and the assault frequency, which are required to find the half-lifetime. The preformation probability is then calculated for each parent nucleus using the experimental Q values and α-decay half lives [40,41]. The preformation factor may be considered as the overlap of the actual ground-state configuration and the configuration representing the α coupled to the ground state of the daughter. Obviously it is expected to be much less than unity [23–26].

In the present calculation, we select the even-even nuclei to study the preformation probability. First, Po isotope chains are chosen. Figure 1 shows the variation of the preformation probability, S_α, with the neutron number, N, for Po isotopes calculated using three Paris-type NN forces BDM3Y1, CDM3Y1, and DDM3Y1. These forces correspond to different values of the nuclear matter incompressibility coefficients $K = 270$, 188, and 176 MeV, respectively [42]. Figure 1 shows that each force produces the same behavior of S_α with N; a clear minimum occurs at $N = 126$, which is a neutron magic number. The preformation probability increases strongly and almost linearly for $N > 126$. This is because the large gap above the magic number enhances the value of the preformation probability. The nucleus tends to get rid of the nucleons in the proton and neutron levels above magic numbers. For $N < 126$, S_α increases slowly, reaching about 0.1 at $N = 112$, then decreases for $N < 112$. As the value of K increases, the value of S_α predicted by the NN force decreases. The largest preformation probability predicted by CDM3Y1 and DDM3Y1 forces is about 0.2, while for BDM3Y1 it has a value of about 0.14. Table I lists the detailed calculations of α decay for Po isotopes using the three different NN interactions.

Our results are comparable to other values. For example, our calculated value of S_α for ^{212}Po α emission is 0.061 using BDM3Y1 NN interactions, to be compared with 2.5×10^{-2}

TABLE I. The preformation probability, S_α, and the α-decay half-lives, $T_{1/2}^{\rm calc}$, calculated without S_α, for Po isotopes using three different NN interactions. Experimental Q values and α-decay half-lives are taken from Refs. [40,41].

Parent nucleus		Expt.		BDM3Y1-Paris		CDM3Y1-Paris		DDM3Y1-Paris	
Z	A	$Q_\alpha^{\rm exp}$ (MeV)	$T_{1/2}^{\rm exp}$ (s)	$T_{1/2}^{\rm calc}$ (s)	S_α	$T_{1/2}^{\rm calc}$ (s)	S_α	$T_{1/2}^{\rm calc}$ (s)	S_α
84	188	8.082	4.3×10^{-4}	1.30×10^{-5}	0.030	1.70×10^{-5}	0.039	1.74×10^{-5}	0.041
84	190	7.693	2.5×10^{-3}	1.74×10^{-4}	0.070	2.27×10^{-4}	0.091	2.34×10^{-4}	0.094
84	192	7.319	3.3×10^{-2}	2.60×10^{-3}	0.079	3.42×10^{-3}	0.104	3.52×10^{-3}	0.107
84	194	6.987	3.9×10^{-1}	3.44×10^{-2}	0.088	4.54×10^{-2}	0.116	4.67×10^{-2}	0.120
84	196	6.657	5.9×10^{0}	5.52×10^{-1}	0.094	7.30×10^{-1}	0.124	7.52×10^{-1}	0.127
84	198	6.309	1.9×10^{2}	1.34×10^{1}	0.070	1.79×10^{1}	0.094	1.85×10^{1}	0.097
84	200	5.981	6.2×10^{3}	3.32×10^{2}	0.054	4.47×10^{2}	0.072	4.61×10^{2}	0.074
84	202	5.701	1.4×10^{5}	7.15×10^{3}	0.051	9.81×10^{3}	0.070	1.01×10^{4}	0.072
84	204	5.485	1.9×10^{6}	8.25×10^{4}	0.043	1.17×10^{5}	0.062	1.21×10^{5}	0.064
84	206	5.327	1.4×10^{7}	5.07×10^{5}	0.036	7.20×10^{5}	0.051	7.43×10^{5}	0.053
84	208	5.215	9.1×10^{7}	1.86×10^{6}	0.020	2.70×10^{6}	0.029	2.76×10^{6}	0.030
84	210	5.407	1.2×10^{7}	1.70×10^{5}	0.014	2.41×10^{5}	0.020	2.49×10^{5}	0.021
84	212	8.954	3.0×10^{-7}	1.84×10^{-8}	0.061	2.34×10^{-8}	0.078	2.41×10^{-8}	0.080
84	214	7.833	1.6×10^{-4}	1.78×10^{-5}	0.111	2.29×10^{-5}	0.143	2.36×10^{-5}	0.147
84	216	6.906	1.5×10^{-1}	1.93×10^{-2}	0.129	2.53×10^{-2}	0.169	2.61×10^{-2}	0.174
84	218	6.115	1.9×10^{2}	2.71×10^{1}	0.143	3.62×10^{1}	0.191	3.73×10^{1}	0.196

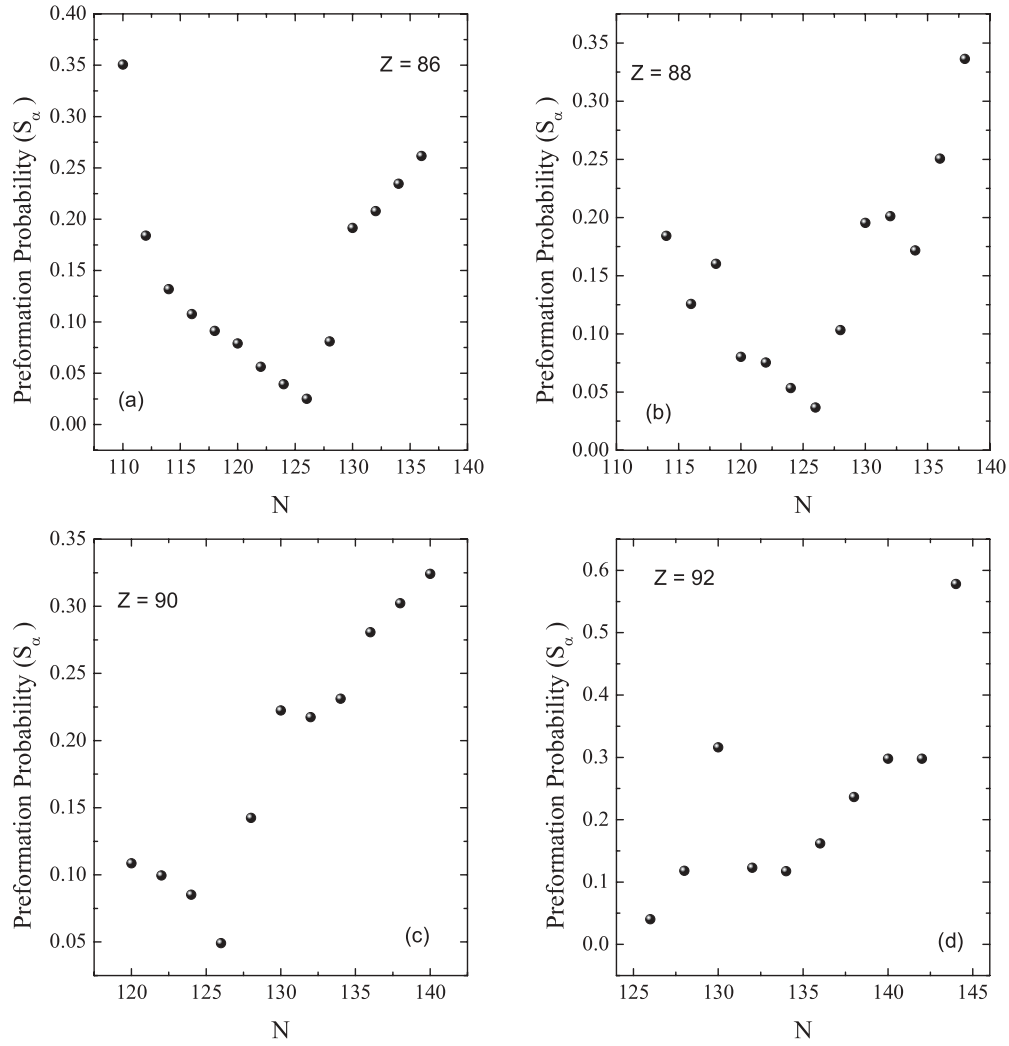

FIG. 2. Extracted α-preformation probability, S_α, for (a) Rn isotopes, (b) Ra isotopes, (c) Th isotopes, and (d) U isotopes using the BDM3Y1-Paris NN interaction with the neutron number, N.

deduced in [26] by a combined shell and cluster model. A value of 3.1×10^{-2} was obtained by Mohr [43] in a double-folding model calculation using the density from the experimentally known charge distribution.

The closer the nucleon number to the magic number, the more difficult α formation in the parent nucleus is. The behavior of S_α in the vicinity of the magic number $N = 126$ for $Z = 86$ isotopes, calculated using BDM3Y1-type force, is shown in Fig. 2(a). The behavior of S_α in this figure is exactly the same as in Fig. 1 except for a sudden increase in S_α, from about 0.18 at $N = 112$ to a value of 0.35 at $N = 110$. This is compared to a small decrease in Fig. 1, from $S_\alpha = 0.094$ at $N = 112$ to $S_\alpha = 0.088$ at $N = 110$. The values of S_α for $Z = 86$ are larger by a factor of about 2 compared to those for Po isotopes.

Clearly the closed shell structures play a key role for the preformation mechanism. The closer the nucleon number to shell closure, the more difficult it is for the α particle to form in the parent nuclei. The dramatic change in the preformation factor around the magic number indicates that the shell effects play an important role in the α formation mechanism in the parent nuclei. Or in other words, the preformation factor can reflect the shell effects.

For the isotopes of the element with $Z = 88$ [shown in Fig. 2(b)], the preformation factors behave with N variation as for elements $Z = 84$ and 86. They have almost the range of values as in Fig. 2(a), except that irregular behavior of S_α appears at $N = 130$, 132, and 134. The behavior around the magic number is the same as in Figs. 1 and 2(a). The same behavior at $N = 130$, 132, and 134 appears for $Z = 90$ as shown in Fig. 2(c). For $Z = 92$, the behavior of S_α against N changes irregularly with increasing N values.

In the following we try to correlate the behavior of the α-decay preformation factor, S_α, with the ground-state energy levels of parent nuclei. For the elements $Z = 84$, 86, 88, 90, and 92, we found that the behavior of S_α around the neutron magic number $N = 126$ is the same for the five elements. S_α increases almost linearly in the vicinity of $N = 126$. S_α varies smoothly for the Po and Rn elements, while it has ripples for the other elements.

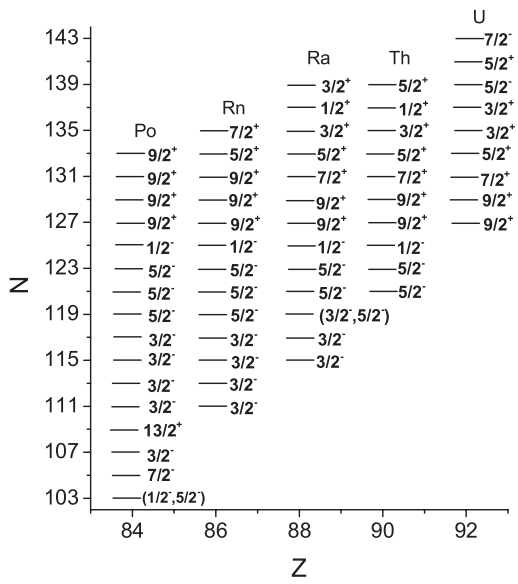

FIG. 3. Schematic representation of the spin and parity, J^π, for Po, Rn, Ra, Th, and U isotopes.

For $N = 127$ of the Po isotope, $J^\pi = 9/2^+$, which means that the neutron level above the neutron closed shell $N = 126$ is the $2g_{9/2}$ single-particle level that can be filled by 10 neutrons. The isotopes of Po nucleus with $N = 129$, 131, and 133 also have $J^\pi = 9/2^+$, as indicated in Fig. 3, and the preformation probability for the Po isotopes with $N = 128$, 130, 132, and 134 increases strongly and regularly with the number of neutrons in the energy level $2g_{9/2}$, as shown in Fig. 1.

The odd-neutron-number Po isotopes with N below the neutron magic number, $N = 126$, have spin and parity $J^\pi = 1/2^-$, $5/2^-$, $3/2^-$, $13/2^+$, and $7/2^-$, as indicated in Fig. 3. The two neutrons in the last filled level for the $N = 126$ Po isotope occupy the $3p_{1/2}$ single-particle level, and the two levels below this one are $2f_{5/2}$ and $3p_{3/2}$, which are filled by 6 and 4 neutrons, respectively. The preformation factor increases slowly and regularly as pairs of neutrons are emitted from these levels (as the neutron number decreases from 126 to 116). For the $N = 114$ Po isotope, the level $3p_{3/2}$ appears as if it is filled again by 4 neutrons, which are emitted, leaving the $N = 110$ Po isotope. The $N = 109$ Po isotope has $J^\pi = 13/2^+$, which means that the pairs of neutrons emitted in α decay from the $N = 110$ Po isotope is from level $1i_{13/2}$, which is filled by 14 neutrons. For this isotope, S_α decreases, compared to the $N = 112$ Po isotope, and it still decreases as N decreases to 104. In the N-variation range (110–104), the spins of the levels of Po isotopes change rapidly and each neutron pair is emitted from a different level.

The behavior of S_α for the Rn isotopes with $110 < N \leqslant 126$ is exactly the same as the corresponding behavior for Po isotopes in the same neutron number range [as shown in Figs. 1 and 2(a); also see Table II]. The levels of odd-neutron-number Rn isotopes in the above neutron range is exactly the same as the corresponding Po isotopes. For $N > 126$, the level $2g_{9/2}$ is repeated three times, as indicated in Fig. 3 (for Rn isotopes with $N = 127$, 129, 131), producing variation of S_α similar to that in Fig. 1, then it is replaced by the levels $5/2^+$ and $7/2^+$ for $N = 133$ and 135, respectively. This level replacement does not affect the behavior of S_α.

TABLE II. The same as Table I, but for Rn, Ra, Th, and U isotopes using the BDM3Y1-Paris NN interaction.

Z	A	$Q_\alpha^{\exp}$ (MeV)	$T_{1/2}^{\exp}$ (s)	$T_{1/2}^{\text{calc}}$ (s)	S_α
86	196	7.617	4.7×10^{-3}	1.65×10^{-3}	0.351
86	198	7.349	6.5×10^{-2}	1.20×10^{-2}	0.184
86	200	7.044	1.0×10^{0}	1.32×10^{-1}	0.132
86	202	6.774	1.2×10^{1}	1.29×10^{0}	0.108
86	204	6.545	1.1×10^{2}	1.00×10^{1}	0.091
86	206	6.384	5.5×10^{2}	4.35×10^{1}	0.079
86	208	6.261	2.4×10^{3}	1.35×10^{2}	0.056
86	210	6.159	9.0×10^{3}	3.55×10^{2}	0.039
86	212	6.385	1.4×10^{3}	3.52×10^{1}	0.025
86	214	9.208	2.7×10^{-7}	2.19×10^{-8}	0.081
86	216	8.200	4.5×10^{-5}	8.62×10^{-6}	0.192
86	218	7.262	3.5×10^{-2}	7.28×10^{-3}	0.208
86	220	6.405	5.6×10^{1}	1.31×10^{1}	0.235
86	222	5.590	3.3×10^{5}	8.63×10^{4}	0.262
88	202	8.020	2.6×10^{-3}	4.79×10^{-4}	0.184
88	204	7.636	5.9×10^{-2}	7.42×10^{-3}	0.126
88	206	7.415	2.4×10^{-1}	3.85×10^{-2}	0.160
88	208	7.273	1.4×10^{0}	1.12×10^{-1}	0.080
88	210	7.152	3.8×10^{0}	2.86×10^{-1}	0.075
88	212	7.032	1.4×10^{1}	7.48×10^{-1}	0.053
88	214	7.273	2.5×10^{0}	9.20×10^{-2}	0.037
88	216	9.526	1.8×10^{-7}	1.86×10^{-8}	0.103
88	218	8.546	2.6×10^{-5}	5.08×10^{-6}	0.195
88	220	7.592	1.8×10^{-2}	3.62×10^{-3}	0.201
88	222	6.697	3.8×10^{1}	6.53×10^{0}	0.172
88	224	5.789	3.3×10^{5}	8.27×10^{4}	0.251
88	226	4.871	5.3×10^{10}	1.78×10^{10}	0.336
90	210	8.053	1.7×10^{-2}	1.85×10^{-3}	0.109
90	212	7.952	3.6×10^{-2}	3.58×10^{-3}	0.100
90	214	7.826	1.0×10^{-1}	8.52×10^{-3}	0.085
90	216	8.071	2.7×10^{-2}	1.33×10^{-3}	0.049
90	218	9.849	1.1×10^{-7}	1.57×10^{-8}	0.142
90	220	8.953	9.7×10^{-6}	2.16×10^{-6}	0.222
90	222	8.127	2.0×10^{-3}	4.35×10^{-4}	0.218
90	224	7.298	1.0×10^{0}	2.31×10^{-1}	0.231
90	226	6.451	1.8×10^{3}	5.05×10^{2}	0.281
90	228	5.520	6.0×10^{7}	1.81×10^{7}	0.302
90	230	4.770	2.4×10^{12}	7.78×10^{11}	0.324
92	218	8.786	1.5×10^{-3}	6.04×10^{-5}	0.040
92	220	10.30	6.0×10^{-8}	7.09×10^{-9}	0.118
92	222	9.500	1.4×10^{-6}	4.43×10^{-7}	0.316
92	224	8.620	7.0×10^{-4}	8.60×10^{-5}	0.122
92	226	7.701	5.0×10^{-1}	5.87×10^{-2}	0.117
92	228	6.803	8.0×10^{2}	1.29×10^{2}	0.162
92	230	5.993	2.7×10^{6}	6.39×10^{5}	0.237
92	232	5.414	3.2×10^{9}	9.53×10^{8}	0.298
92	234	4.858	7.7×10^{12}	2.29×10^{12}	0.298
92	236	4.573	7.4×10^{14}	4.28×10^{14}	0.578

TABLE III. The same as Table II, but for heavier nuclei in recent experiments [47–53] including new data with improved accuracy.

Parent nucleus		Expt.		BDM3Y1-Reid		BDM3Y1-Paris	
Z	A	$Q_\alpha^{\rm exp}$ (MeV)	$T_{1/2}^{\rm exp}$	$T_{1/2}^{\rm calc}$	S_α	$T_{1/2}^{\rm calc}$	S_α
118	294	11.81(6)	$0.89^{+1.07}_{-0.31}$ ms	0.088 ms	0.099	0.081 ms	0.091
117	294	10.96(10)	78^{+370}_{-36} ms	4.507 ms	0.058	4.139 ms	0.05
117	293	11.18(8)	14^{+11}_{-4} ms	1.316 ms	0.094	1.208 ms	0.086
115	289	10.45(9)	$0.22^{+0.26}_{-0.08}$ s	0.023 s	0.106	0.022 s	0.098
114	289	10.01(3)	$2.1^{+0.8}_{-0.4}$ s	0.172 s	0.082	0.158 s	0.075
114	288	10.09(3)	$0.69^{+0.17}_{-0.11}$ s	0.105 s	0.152	0.097 s	0.140
113	285	9.88(8)	$5.5^{+5.0}_{-1.8}$ s	0.200 s	0.036	0.184 s	0.034
112	285	9.34(3)	29^{+11}_{-6} s	3.503 s	0.121	3.223 s	0.111
110	281	8.88(3)	144^{+250}_{-12} s	20.696 s	0.144	19.050 s	0.132
108	265	10.588(15)	$1.7^{+1.7}_{-0.6}$ ms	0.089 ms	0.052	0.082 ms	0.048
108	263	11.06(6)	$0.74^{+0.48}_{-0.21}$ ms	0.007 ms	0.010	0.007 ms	0.009
107	262	9.839(15)	83 ± 14 ms	3.776 ms	0.045	3.473 ms	0.042
107	261	$\simeq$10.16	$11.8^{+3.9}_{-2.4}$ ms	0.547 ms	0.046	0.503 ms	0.043
106	267	8.32(5)	471 s	68.409 s	0.145	63.007 s	0.134
106	265	8.82(5)	15^{+7}_{-4} s	1.494 s	0.100	1.376 s	0.092
106	260	9.900(10)	4.95 ± 0.33 ms	1.216 ms	0.246	1.119 ms	0.226
105	257	9.300(20)	0.67 ± 0.6 s	0.028 s	0.041	0.025 s	0.038
103	253	8.859(20)	1.32 ± 0.14 s	0.116 s	0.088	0.107 s	0.081
101	249	8.157(10)	23 ± 3 s	4.155 s	0.181	3.828 s	0.1664
98	237	8.220(20)	1.14 ± 0.29 s	0.230 s	0.202	0.212 s	0.186
96	236	7.074(20)	2278 ± 278 s	521.601 s	0.229	481.272 s	0.211
96	233	7.473(20)	164^{+93}_{-43} s	16.487 s	0.101	15.210 s	0.093

For the odd-neutron-number Ra isotopes [Fig. 2(b)], with $N > 126$, the level $2g_{9/2}$ is repeated twice, producing the same regular behavior in S_α, then the order of levels change after every emitted neutron pair, producing irregular behavior in S_α at $N = 132$ and 134. The level $2g_{9/2}$ is still occupied by 6 neutrons. The same happens for $N < 126$, where the level $2f_{5/2}$ did not emit all its neutrons and irregular behavior of S_α occurs at $N = 118$.

Figures 2(c) and 2(d) for the variation of S_α with the neutron number for Th and U isotopes, respectively, reflect the same correlation between the behavior of S_α and the energy levels of the parent nucleus. This correlation has the following characteristics:

(i) For specific isotope, the α-decay preformation probability (S_α) increases almost linearly with an increase in the number of neutrons above the neutron magic number $N = 126$ if the neutron pair of α particle is emitted from one single level. This is clear in Figs. 1 and 2(a)–2(d) from the behavior of S_α for $N \geqslant 126$ when the neutrons are emitted from the level $2g_{9/2}$.

(ii) For $N \leqslant 126$, a number of neutron single-particle energy levels with small occupation numbers such as $3p_{1/2}$, $2f_{5/2}$, and $3p_{3/2}$ contribute to α decay. S_α increases regularly with an increase in the number of neutron holes in levels below $N = 126$ assuming that the order of levels does not change during the emission process and the upper level emits all its neutrons. The increase in S_α, in this case, is slower than the emission of a single level in the $N > 126$ case. As an example, the α decay for isotopes of Po and Rn with neutron numbers $N = 124$, 122, and 120 in Figs. 1 and 2(a) is from the neutron level $2f_{5/2}$. Also, for $N = 118$, 116, 114, and 112 in Po and Rn isotopes, the α particle is emitted from the level $3p_{3/2}$, which contributes to the α decay when level $2f_{5/2}$ becomes empty. Note that level $3p_{3/2}$ is filled, leaving four holes in a lower level.

(iii) Irregular behavior, a ripple, or a decrease in preformation probability occurs if the levels of the parent nucleus change after each α emission process or holes are present in the lower levels.

We have extended our calculations of the preformation probability of α decay to the recently synthesized heavy and SHN. The synthesis of new superheavy elements is a hot and attractive topic. The isotopes of elements 112, 114, 116, and ^{294}118 have been produced by irradiations of ^{233,238}U, ^{242}Pu, ^{248}Cm, and ^{249}Cf targets with a ^{48}Ca beam at various energies in the fusion evaporation reactions [44,45]. The very recent synthesis of the new isotopes ^{293,294}117 [46,47] fills the final gap to $Z = 118$ in the nuclide chart. Given that α decay is the primary decay mode of SHN, the observation of α-decay

chains has been a reliable tool to identify new SHN and new isomeric states. The new experiments in Darmstadt, Berkeley, and Dubna [47–53] provide a perfect opportunity to test the present α-decay study strictly, and this study may in turn check whether these measured values, such as decay energies and half-lives, in these α-decay chains are consistent with each other to some extent. Detailed numerical results for the newly observed α-decay of heavier nuclei are listed in Table III. It should be noted that odd-A SHN have nonzero spins and spin-parity conservation might force an α particle to carry away nonzero angular momentum. However, we assume that all α transitions between the ground states of parent and daughter SHN took place at $\ell = 0$, owing to nonavailability of the spin parities of these nuclei [22]. The experimental error bar is also relatively large in the measurement of decay energies and half-lives owing to experimental difficulties and the paucity of observed decay events. Various model calculations including the DDM3Y with a zero-range exchange interaction [30] have focused on the new SHN. Now the preformation probability is calculated using the realistic density-dependent NN interaction, BDM3Y1, of Reid and Paris types together with their experimental data on α-decay half-lives and Q values [47–53]. The results are reported in Table III. One can see that the orders of half-lives range from milliseconds to seconds. These results indicate that SHN are weakly bound, and such nuclei will quickly decay through α emission when synthesized.

IV. CONCLUSION

In summary, we investigated the dependence of the preformation probability, spectroscopic factor, of an α cluster on the neutron number. The main effect of antisymmetrization under exchange of nucleons between the α and the daughter nuclei has been included in the folding model through the finite-range exchange part of the NN interaction. The variation of S_α with the neutron number for the isotopes of Po, Rn, Ra, Th, and U elements is studied around the neutron magic number $N = 126$.

The study clarifies that it is difficult to form an α cluster in the parent nuclei when the nucleon number is close to the magic number. Moreover, we have found a strong correlation between the behavior of S_α with the variation in neutron number and spins of adjacent odd-neutron-number isotopes. S_α shows a regular behavior with the neutron number if the neutron pair of α particles, emitted from adjacent isotopes, comes from the same energy level or from a group of levels, assuming that the order of levels in this group is not changed. Irregular behavior of S_α with the neutron number occurs if the levels of the adjacent isotopes change or holes are present in lower levels.

The calculations extending to the recently synthesized SHN show that they are weakly bound. They quickly decay through emission of α clusters when synthesized.

[1] S. Hofmann and G. Munzenberg, Rev. Mod. Phys. **72**, 733 (2000).
[2] P. E. Hodgeson and E. Betak, Phys. Rep. **374**, 1 (2003).
[3] R. G. Lovas, R. J. Liotta, A. Insolia, K. Varga, and D. S. Delion, Phys. Rep. **294**, 265 (1998).
[4] D. Seweryniak, K. Starosta, C. N. Davids, S. Gros, A. A. Hecht, N. Hoteling, T. L. Khoo, K. Lagergren, G. Lotay, D. Peterson, A. Robinson, C. Vaman, W. B. Walters, P. J. Woods, and S. Zhu, Phys. Rev. C **73**, 061301(R) (2006).
[5] H. J. Mang, Annu. Rev. Nucl. Sci. **14**, 1 (1964).
[6] S. Hofmann *et al.*, Eur. Phys. J. A **10**, 5 (2001).
[7] Yu. Ts. Oganessian *et al.*, Phys. Rev. C **74**, 044602 (2006).
[8] S. Hofmann, Rep. Prog. Phys. **61**, 639 (1998).
[9] K. Morita, K. Morimoto, D. Kaji, T. Akiyama, Sin-ichi Goto, H. Haba, E. Ideguchi, R. Kanungo, K. Katori, H. Koura, H. Kudo, T. Ohnishi, A. Ozawa, T. Suda, K. Sueki, H. Xu, T. Yamaguchi, A. Yoneda, A. Yoshida, and Y. Zhao, J. Phys. Soc. Jpn. **73**, 2593 (2004).
[10] Yu. Ts. Oganessian, A. G. Demin, A. S. Iljnov *et al.*, Nature **400**, 242 (1999).
[11] Yu. Ts. Oganessian, V. K. Utyonkov, Yu. V. Lobanov *et al.*, Phys. Rev. C **62**, 041604(R) (2000).
[12] Yu. Ts. Oganessian, V. K. Utyonkov, Yu. V. Lobanov *et al.*, Phys. Rev. C **69**, 021601(R) (2004).
[13] G. Gamow, Z. Phys. **51**, 204 (1928).
[14] J. Dong, H. Zhang, Y. Wang, W. Zuo, and J. Li, Nucl. Phys. A **832**, 198 (2010).
[15] C. Xu and Z. Z. Ren, Nucl. Phys. A **753**, 174 (2005).
[16] V. Yu. Denisov and A. A. Khudenko, Phys. Rev. C **80**, 034603 (2009).
[17] K. P. Santhosh and A. Joseph, Pramana J. Phys. **58**, 611 (2002).
[18] G. Wentzel, Z. Phys. **38**, 518 (1926).
[19] B. Buck, A. C. Merchant, and S. M. Perez, Phys. Rev. C **51**, 559 (1995).
[20] S. B. Duarte and N. Teruya, Phys. Rev. C **85**, 017601 (2012).
[21] M. Ismail, A. Y. Ellithi, M. M. Botros, and A. Adel, Phys. Rev. C **81**, 024602 (2010).
[22] Y. Qian and Z. Ren, Phys. Rev. C **84**, 064307 (2011).
[23] G. L. Zhang, X. Y. Le, and H. Q. Zhang, Nucl. Phys. A **823**, 16 (2009).
[24] H. F. Zhang, J. M. Dong, G. Royer, W. Zuo, and J. Q. Li, Phys. Rev. C **80**, 037307 (2009).
[25] W. M. Seif, M. Shalaby, and M. F. Alrakshy, Phys. Rev. C **84**, 064608 (2011).
[26] K. Varga, R. G. Lovas, and R. J. Liotta, Phys. Rev. Lett. **69**, 37 (1992).
[27] D. T. Khoa and W. von Oertzen, Phys. Lett. B **342**, 6 (1995).
[28] M. Ismail, M. M. Osman, and F. Salah, Phys. Rev. C **60**, 037603 (1999).
[29] D. T. Khoa, Phys. Rev. C **63**, 034007 (2001).
[30] P. R. Chowdhury, C. Samanta, and D. N. Basu, Phys. Rev. C **73**, 014612 (2006).
[31] M. Ismail and W. M. Seif, Phys. Rev. C **81**, 034607 (2010).
[32] B. Sinha, Phys. Rep. **20**, 1 (1975).
[33] B. Sinha and S. A. Moszkowski, Phys. Lett. B **81**, 289 (1979).
[34] G. R. Satchler and W. G. Love, Phys. Rep. **55**, 183 (1979).
[35] X. Campi and A. Bouyssy, Phys. Lett. B **73**, 263 (1978).
[36] C. Xu and Z. Ren, Phys. Rev. C **74**, 014304 (2006).
[37] C. Xu and Z. Ren, Phys. Rev. C **73**, 041301(R) (2006).
[38] N. G. Kelkar and H. M. Castaneda, Phys. Rev. C **76**, 064605 (2007).
[39] M. Bhattacharya, S. Roy, and G. Gangopadhyaya, Phys. Lett. B **665**, 182 (2008).

[40] G. Audi, A. H. Wapstra, and C. Thibault, Nucl. Phys. A **729**, 337 (2003).
[41] J. C. Pei, F. R. Xu, Z. J. Lin, and E. G. Zhao, Phys. Rev. C **76**, 044326 (2007).
[42] D. T. Khoa, G. R. Satchler, and W. von Oertzen, Phys. Rev. C **56**, 954 (1997).
[43] P. Mohr, Phys. Rev. C **61**, 045802 (2000).
[44] Yu. Ts. Oganessian *et al*., Phys. Rev. C **70**, 064609 (2004).
[45] Yu. Ts. Oganessian *et al*., Phys. Rev. C **71**, 029902(E) (2005).
[46] Yu. Ts. Oganessian *et al*., Phys. Rev. Lett. **104**, 142502 (2010).
[47] Yu. Ts. Oganessian *et al*., Phys. Rev. C **83**, 054315 (2011).
[48] F. P. Heßberger *et al*., Eur. Phys. J. A **41**, 145 (2009).
[49] F. P. Heßberger, S. Antalic, D. Ackermann, S. Heinz, S. Hofmann, J. Khuyagbaatar, B. Kindler, I. Kojouharov, B. Lommel, and R. Mann, Eur. Phys. J. A **43**, 175 (2010).
[50] J. Khuyagbaatar *et al*., Eur. Phys. J. A **46**, 59 (2010).
[51] I. Dragojevic, K. E. Gregorich, Ch. E. Düllmann, J. Dvorak, P. A. Ellison, J. M. Gates, S. L. Nelson, L. Stavsetra, and H. Nitsche, Phys. Rev. C **79**, 011602(R) (2009).
[52] Ch. E. Dullmann *et al*., Phys. Rev. Lett. **104**, 252701 (2010).
[53] J. Dvorak *et al*., Phys. Rev. Lett. **100**, 132503 (2008).